 MCB, vol.6, no.4, pp.191-201, 2009

On the Origins of the Universal Dynamics of Endogenous Granules in Mammalian Cells

Siva A. Vanapalli[*,†], Yixuan Li[†], Frieder Mugele[†] and Michel H. G. Duits[†]

Abstract: Endogenous granules (EGs) that consist of lipid droplets and mitochondria have been commonly used to assess intracellular mechanical properties via multiple particle tracking microrheology (MPTM). Despite their widespread use, the nature of interaction of EGs with the cytoskeletal network and the type of forces driving their dynamics – both of which are crucial for the interpretation of the results from MPTM technique - are yet to be resolved. In this report, we study the dynamics of endogenous granules in mammalian cells using particle tracking methods. We find that the ensemble dynamics of EGs is diffusive in three types of mammalian cells (endothelial cells, smooth muscle cells and fibroblasts), thereby suggesting an apparent universality in their dynamical behavior. Moreover, in a given cell, the amplitude of the mean-squared displacement for EGs is an order of magnitude larger than that of injected particles. This observation along with results from ATP depletion and temperature intervention studies suggests that cytoskeletal active forces drive the dynamics of EGs. To elucidate the dynamical origin of the diffusive-like nonthermal motion, we consider three active force generation mechanisms – molecular motor transport, actomyosin contractility and microtubule polymerization forces. We test these mechanisms using pharmacological interventions. Experimental evidence and model calculations suggest that EGs are intimately linked to microtubules and that microtubule polymerization forces drive their dynamics. Thus, endogenous granules could serve as non-invasive probes for microtubule network dynamics in mammalian cells.

Keyword: Cytoskeleton, microrheology, microtubule polymerization, molecular motor, actin-myosin contractility.

1 Introduction

Cellular function is intimately linked to their mechanical properties (1,2). For example, the ability of cells to crawl and migrate is influenced by their global mechanical properties as quantified by their frequency dependent shear moduli. In addition, cells constantly modify their local mechanical properties by remodeling their internal microstructure (3). This precise control over cellular mechanical behavior is orchestrated by the cytoskeleton – a multifunctional body consisting of dense networks of biopolymers that is being dynamically modulated by a number of active processes driven by a myriad of cytoskeletal proteins and ATP (4).

Recently, significant advances have been made in the understanding of the mechanical behavior of the living cytoskeleton using a variety of techniques including optical tweezers (5), magnetic twisting cytometry (6), atomic force microscopy (7), particle-tracking microrheology (8) and microplate rheometry (9). Among these techniques multiple particle tracking microrheology (MPTM) is a versatile method as both the local and global cellular mechanical properties can be simultaneously determined using probe particles (10,11). In the literature (12-17) naturally present endogenous granules (usually lipid droplets and mitochondria) have been widely used to assess intracellular rheology. In spite of their widespread

[*] Corresponding Author: Present address: Department of Chemical Engineering, Texas Tech University, Lubbock, TX 79409-3121, Email Address: siva.vanapalli@ttu.edu

[†] Physics of Complex Fluids, Department of Science & Technology and MESA+ Institute of Nanotechnology, University of Twente, P. O. Box 217, 7500 AE Enschede, The Netherlands

use, knowledge of the nature of interaction of endogenous granules (EGs) with the cytoskeleton, that underpins the MPTM method is lacking. Recent evidence suggests that the EGs are sensitive to non-thermal intracellular stress fluctuations (11). However, neither the microscopic origin of these active forces nor the concomitant cytoskeletal biopolymers that drive the motion of endogenous granules have been identified. In this study, we investigate the motion of endogenous granules under a variety of pharmacological conditions and report the first evidence that the dynamics of endogenous granules is intimately linked to the microtubule polymerization forces.

2 Materials and methods

2.1 Cell Culture and intracellular probes

Human microvascular endothelial cells (HMECs), human umbilical vein smooth muscle cells and COS-7 African green monkey kidney fibroblasts were cultured at 37°C in a humidified 5% CO_2 environment. Cells were plated on a Delta T culture dish (Bioptechs, Butler, PA, USA), precoated with fibronectin (100 μg/mL solution). The endogenous granules were identified to be lipid droplets and mitochondria by staining with nile red and rhodamine dyes respectively. The mean diameter of the granules was assessed to be $\approx$ 0.5 μm. The injected particles were carboxylated fluorescent polystyrene beads of 200 nm in size and were introduced ballistically into the cells using a Biolistic gun (He/PS 1000, Bio-Rad) according to the protocol of Panchoran et al. (18).

2.2 Interventions

All drugs were purchased from Sigma Aldrich, except blebbistatin (Tebu-bio, Belgium). Drug intervention studies were performed only with endothelial cells and the following drugs were used: Latrunculin A (200 nM, 2hrs), Blebbistatin (50 μM, 2hrs), Jasplakilonide (25 nM, 1hr), Nocodazole (5 μM, 3hrs) and Cephalomannine (taxol, 100 μM, 1hr). For ATP depletion, 2-D-deoxyglucose and sodium azide at final concentrations of 50 mM and 0.05% were respectively used for 30 mins. To study temperature effects, the Bioptechs heating system was used to modulate the temperature of the cells between 37 °C and 24 °C allowing for a 30 min waiting period. For all drug intervention experiments ten endothelial cells were tracked over a period of 2-3 hrs.

2.3 Multiple particle tracking experiments

Probe particles were visualized using a spinning-disk inverted confocal microscope (UltraView LCI 10, Perkin Elmer, Cambridge, UK). Endogenous granules were imaged under phase contrast mode using a 100 X (NA 1.3) objective, while ballistically injected particles were visualized under fluorescence mode. Approximately, 2500 images were recorded with a 12-bit CCD camera (Hamamatsu, Bridgewater, NJ) at $\sim$17 frames per second for a typical duration of 150 seconds. The spatial resolution corresponding to the images was 0.13 μm per pixel. In each cell, 50-100 EGs and 15-40 BIPs were tracked. The particles were identified using the publicly available particle-tracking code based on the paper by Crocker and Grier (19), written and extended in Interactive Data Language (IDL, Visual Information Solutions, Boulder, CO) by several authors (see acknowledgement).

We now discuss the errors associated with our particle-tracking experiments. The error in our particle displacements was measured to be $\approx$ 6-10 nm by tracking immobilized particles. To assess the bias associated with sampling more of the trajectories corresponding to slowly moving particles, we performed block analysis of the images. A single run of 2500 images containing EGs in an endothelial cell was split up into blocks of 300 images and the calculated ensemble-averaged mean-squared displacement was found to be indistinguishable for the various block data sets. To assess the extent of inaccuracy introduced in our data by slow processes (e.g. cell crawling), we recorded four consecutive movies of EGs in the same endothelial cell over a period of 30 minutes. We found the mean squared displacement (MSD) curves to exhibit similar temporal response with amplitude variation of $\approx$10-20%.

We associate molecular motor transport with

superdiffusive behavior (20-22) i.e. where the power-law exponent corresponding to MSD curves is greater than unity. To identify molecular motor transport (i.e. superdiffusive) behavior in the dynamics of EGs we gathered 10000 single particle (granule) trajectories. We calculated the power-law exponent corresponding to single particle MSDs and generated power-law exponent distributions. We assessed the statistical significance of these distributions by comparing it against Brownian particle simulations (23). In our simulations for Brownian systems, power-law exponents below or above 1.0 were obtained occasionally for trajectory lengths comparable to our experiments, probably due to finite trajectory lengths. This finding indicates that based on the power-law exponent alone, it is not generally possible to tag individual particle trajectories as superdiffusive. We therefore generated power-law exponent distributions and in instances where we observed a portion of the distribution to lay outside the Brownian particle distribution, we attributed it to be statistically significant.

3 Results & discussions

3.1 Universal diffusive dynamics of endogenous granules are driven by cytoskeletal active forces

Figure 1 shows the ensemble mean-squared displacement of endogenous granules analyzed from ten different endothelial cells. We find that in spite of cell to cell amplitude variation in MSD, the temporal response shows a power-law slope close to 1. We use the term diffusive to describe this behavior because of the powerlaw slope of unity. We also tracked endogenous granules in other cell types to verify if this diffusive behavior persists. Figure 2 reports the mean-squared displacement (MSD) of endogenous granules in three different mammalian cell lines – endothelial cells ($\alpha = 0.90 \pm 0.01$), smooth muscle cells ($\alpha = 0.83 \pm 0.01$) and fibroblasts ($\alpha = 0.94 \pm 0.01$). Here α is the exponent derived form power-law fit to the data. Remarkably, we find that the dynamics of EGs in all three types of cells is nearly diffusive over the time-scales probed. Similar diffusive behavior has also been observed in macrophages and carcinoma cells (11), but in yeast (14) and amoeba (17), subdiffusive behavior was found. These observations suggest that the diffusive dynamics of endogenous granules might be a universal characteristic of mammalian cells.

To assess whether the observed universal diffusive behavior of endogenous granules is driven by passive (thermal) or active (non-thermal) forces we used two approaches. First, we studied the effect of active motion interventions - lowering the temperature and ATP depletion - on the ensemble dynamics of EGs. We find that both the treatments reduce the amplitude of the MSD (see Fig. 3) to similar values, with temperature reduction and ATP depletion yielding $\alpha = 0.76 \pm 0.04$ and 0.66 ± 0.03 respectively. These results suggest that cytoskeletal active forces play a central role in determining the dynamics of endogenous granules.

Second, we performed independent particle tracking experiments with ballistically injected particles (BIPs) and compared their MSD against that of EGs. Remarkably, we find that, although BIPs are about half the size of EGs, their amplitude of MSD is about an order of magnitude smaller than that of EGs, This amplitude difference persists in spite of cell-to-cell variability. To further validate these remarkable differences in the ensemble dynamics of EGs and BIPs, we analyzed an additional set of five cells containing *both* EGs and BIPs. Again, the large difference between the amplitudes of the MSDs for the two probes was observed. Since ballistically injected particles have been previously reported to behave as passive probes in living cells (18), we attribute the enhanced amplitude in the MSD of EGs compared to BIPs to active cytoskeletal forces.

3.2 Probing the origins of the non-equilibrium dynamics of endogenous granules

We now probe the origins of the diffusive dynamics of endogenous granules that appears to be a generic feature of mammalian cells and is being driven by non-equilibrium fluctuations. A major contributor to non-equilibrium motion in living cells are ATP-driven active processes (11). At the

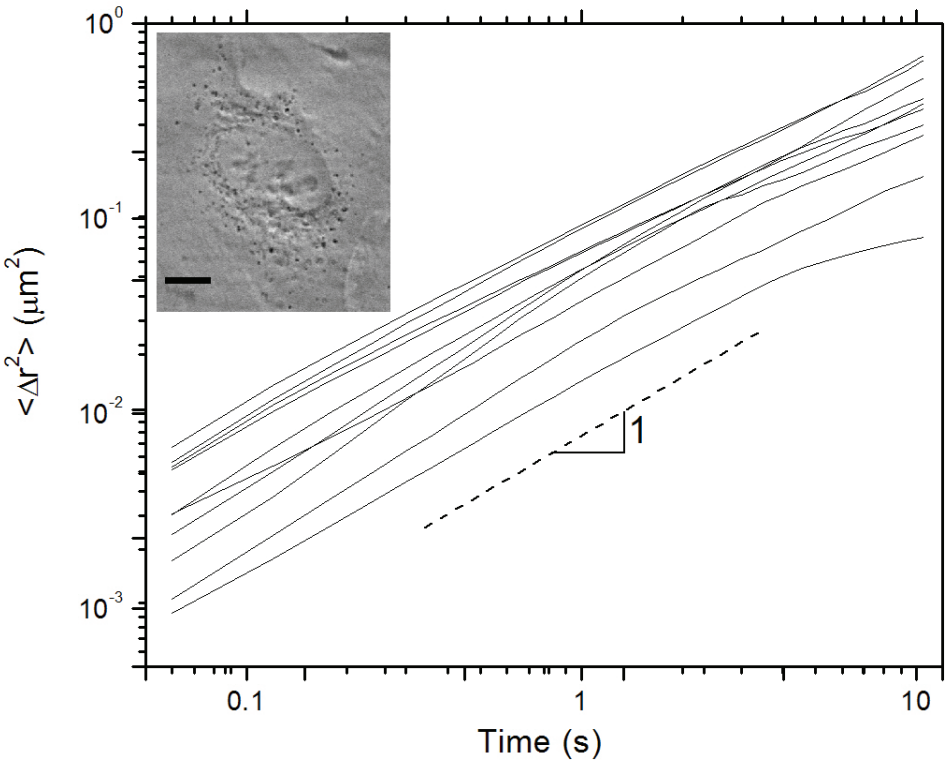

Figure 1: Ensemble dynamics of endogenous granules in endothelial cells (HMEC-1) at 37 °C. The lines are the ensemble-averaged mean-squared displacement of EGs for ten individual cells. Inset shows phase contrast image of an endothelial (HMEC-1) cell with the dark objects being endogenous granules. Scale bar is 10 μm.

molecular level there could be many sources of ATP-driven activity in living cells, however from the perspective of cellular mechanical force generation, we consider three known candidates for intracellular active behavior.

3.2.1 Molecular motor driven transport

Intracellular active transport arises from interaction of either kinesin and dynein motors with microtubules or myosins with actin filaments. In both cases, this type of cargo-transport behavior has been shown to result in superdiffusive behavior (20-22). We analyze the single-particle trajectories of EGs (c.f. Section 2.3) and indeed observe super-diffusive behavior as shown in Figure 4. However, the fraction of EGs exhibiting such intracellular transport is rather small. Eliminating the statistically significant superdiffusive trajectories ($\alpha > 1.2$ as per fig.4) and re-analyzing the data (not shown), we still find the dynamics of EGs to be predominantly diffusive. Therefore it is unlikely that the ensemble dynamics of endogenous granules is being driven simply by intracellular transport coupled to motor protein activity.

3.2.2 Actomyosin contractility

Contractile mechanical forces are generated in living cells via actin-myosin interactions, where the myosin II motor cross-links and slides on actin filaments. Here we consider if such actin-myosin contractile forces are important for the observed diffusive dynamics of endogenous granules. This hypothesis has been motivated by a recent *in vitro* study (24) involving a composite network of actin filaments, microtubules and myosin II motors that has shown motor-induced non-thermal fluctuations to be diffusive-like. To test this hypothesis *in vivo* we subjected the endothelial cells to latrunculin, blebbistatin and jaspakilonide drug interventions. Latrunculin (LA) binds

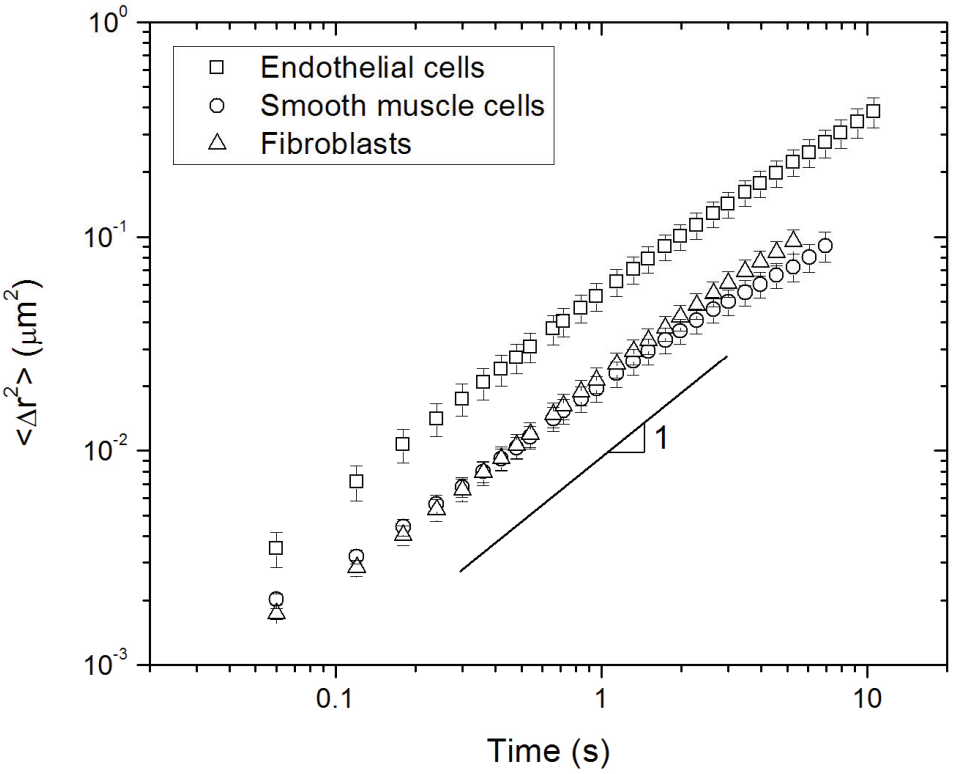

Figure 2: Mean squared displacement of endogenous granules versus lag time at 37 °C for three different kinds of mammalian cells. The symbols represent the average over N = 10, 5 and 6 cells for endothelial cells, smooth muscle cells and fibroblasts respectively. The error bars are standard errors.

to actin monomers and inhibits the polymerization of actin filaments, implying that the associated actin binding proteins (including myosin isoforms) are presumably inactivated as well. Blebbistatin specifically disrupts the activity of the myosin II motor and jasplakinolide stabilizes the actin network by inducing actin polymerization.

In Figure 5 we show that the LA intervention does not significantly alter the MSD of endogenous granules, although from the cell morphology and immunofluorescene staining of the actin network (data not shown) we observe that LA was active and efficient. This observation suggests that the intracellular actin network does not affect the dynamics of endogenous granules. Contrary to the above conclusion, both blebbistatin and jasplakinolide interventions yield an MSD amplitude and slope that is different from that of EGs in the untreated cells. We reconcile this apparent discrepancy and discuss the importance of actin-myosin contractility for EG dynamics in Section 3.3.

3.2.3 Microtubule bending forces

Non-equilibrium microtubule bending modes in living cells could arise either from acto-myosin contractility (24) or from microtubule polymerization forces (25). Here, we consider the bending dynamics of microtubules driven by non-thermal forces as a possible source of diffusive dynamics of EGs. This hypothesis has been motivated by a recent direct observation of intracellular microtubule tip growth dynamics, which was found to be diffusive-like and ATP dependent (25). To test this hypothesis we subjected endothelial cells to nocodazole and taxol drug interventions. Nocodazole binds to beta-tubulin and prevents microtubule polymerization, while taxol promotes the assembly of stable microtubules from alpha and beta tubulin and inhibits their depolymerization. In Figure 5, we show that both nocodazole and taxol dramatically reduce the amplitude of MSD,

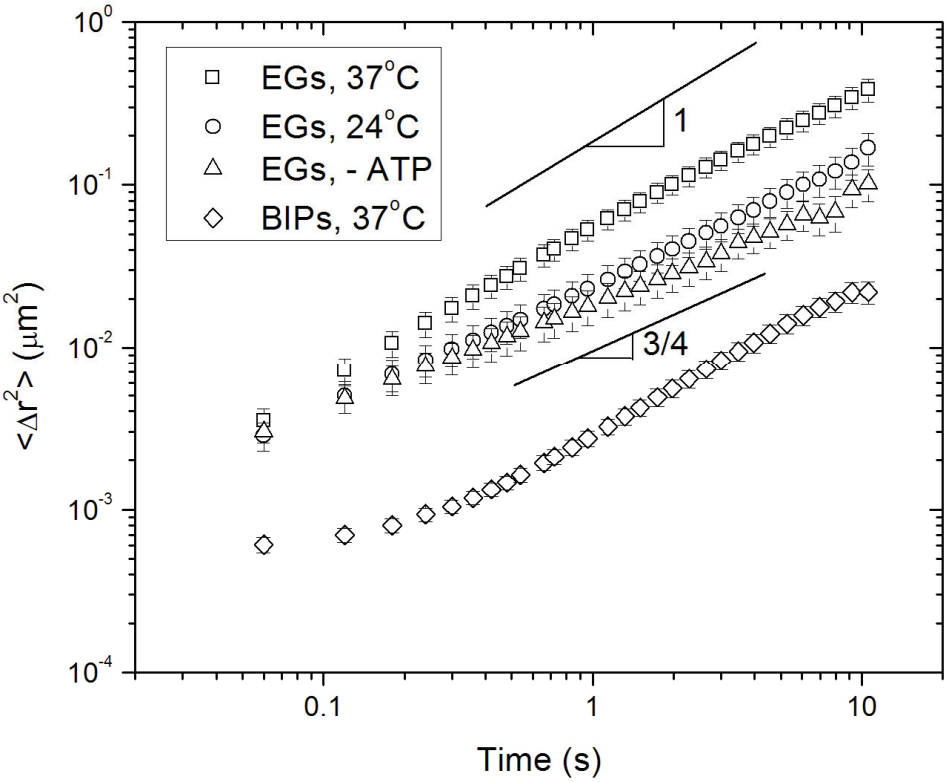

Figure 3: Influence of ATP depletion and reduction in temperature on the ensemble dynamics of endogenous granules in endothelial cells. Also shown is the mean-squared displacement of ballistically injected particles. The error bars are standard errors calculated from data acquired on ten endothelial cells.

indicating that microtubules are an important cytosleketal element affecting the dynamics of EGs.

3.3 *Microtubule polymerization dynamics drives the motion of endogenous granules in mammalian cells*

In the previous section, we assessed possible mechanistic origins of endogenous granule dynamics. In this section, we begin with two model calculations that support the notion that microtubules play a crucial role in determining the dynamics of EGs. The first model analysis estimates the amplitude of the MSD experienced by endogenous granules linked to thermally driven microtubules. The second model links actively driven microtubule bending dynamics to endogenous granule motion. We use this model subsequently to explain the observed effects of drug interventions (c.f. Fig. 5) on EG dynamics.

Monomer fluctuations due to thermal energy in a semiflexible polymer network have been shown both experimentally and theoretically (26, 27) to obey a unique scaling of the form

$$\begin{aligned}\left\langle \Delta r_o^2 \right\rangle &= At^{3/4} \\ &= 0.41\left[\ln\left(\frac{\kappa t \ln(L/\pi a)}{4\pi\eta a^4}\right)\right]\frac{k_B T}{\eta^{3/4}\kappa^{1/4}}t^{3/4} \end{aligned} \quad (1)$$

In Eqn (1) k_BT is thermal energy, η is solvent viscosity, L is the polymer contour length, a is the chain diameter and κ is the bending rigidity. In our active motion intervention experiments, especially under temperature reduction to 24 °C (c.f. Figure 3), we observe a power-law exponent of $\sim$ 3/4 for EG dynamics. Assuming EGs are linked to a semiflexible polymer network, we assess which of the semiflexible polymer networks in living cells - actin filament (AF), microtubule (MT) or intermediate filament (IF) networks - yield an estimate of the prefactor A that is comparable with temperature reduction experiment. For

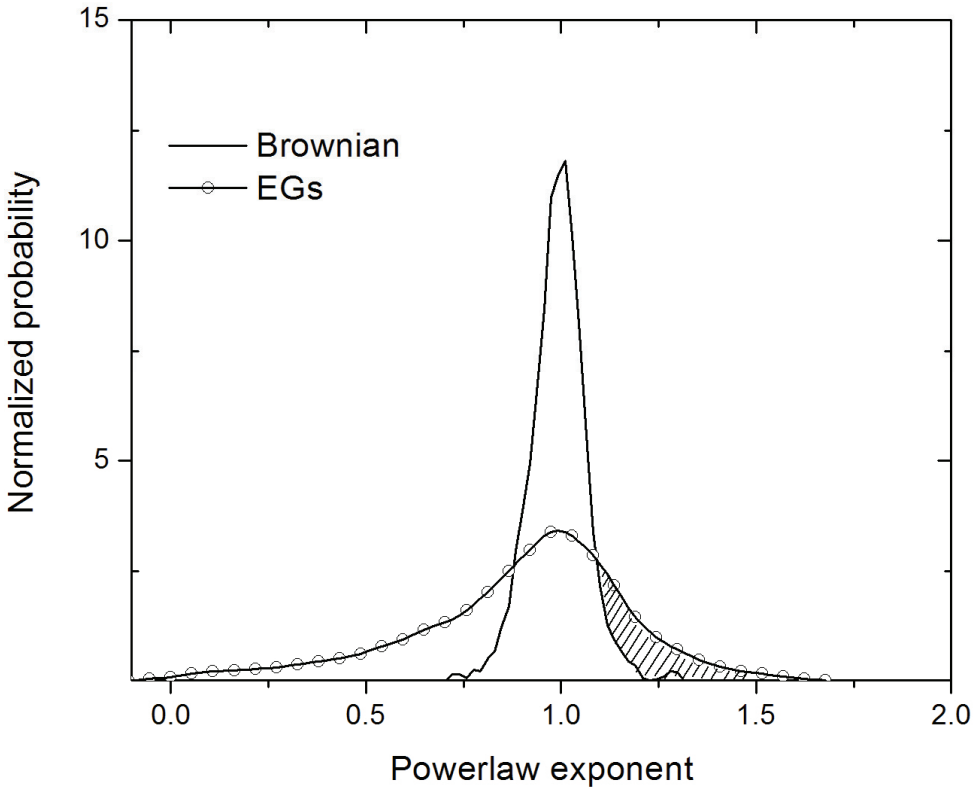

Figure 4: Probability distributions of the power-law exponents corresponding to single-particle trajectories for endogenous granules in endothelial cells compared against Brownian particles. The hatched area denotes the statistically significant population of EGs that show superdiffusive behavior.

this calculation, we take η = 0.1 Pa.s (2), L = 1 μm. The values of κ for the AF, MT and IF are 7×10^{-26}, $2\times10^{-23}$and 4×10^{-27}Nm^2 respectively (1,28). The corresponding chain diameters are 2.5, 15 and 10 nm (1,28). We find that $A \approx$ 0.42, 0.09 and 0.52 μm^2/s$^{3/4}$ for AF, MT and IF networks respectively. From Fig. 3, we determine a prefactor of 0.02 μm^2/s$^{3/4}$ that is closest to the predicted value for microtubules rather than for actin or intermediate filaments. Thus, this analysis suggests that endogenous granule motion is driven by microtubules.

We now estimate the magnitude of non-thermal forces driving EG dynamics assuming that EGs experience the transverse bending modes due to microtubule buckling as shown in Figure 6. Our analysis is based on recent literature models (25, 29-31) that consider a microtubule of bending rigidity, κ, undergoing buckling in an (isotropic, homogeneous and linear) elastic medium of modulus, G, due to a motor-driven compressional force, f. We briefly discuss this model for the sake of completeness. When a compressional point force due to a motor protein is imposed as shown in Figure 6, unlike classical long-wavelength Euler buckling the microtubule undergoes short-wavelength buckling. This is because, in the presence of an elastic medium, for the same end-to-end compression, the short wavelength buckling is energetically more favorable than long-wavelength Euler buckling. This microtubule buckling behavior can be described by a characteristic longitudinal and transverse length scales of order l_o and h_o respectively. To link the compression force f to the microtubule deflections, we consider the energy associated with the buckling behavior. The bending energy along the length of the microtubule is given by

$$\int \kappa \left(\frac{d^2u}{dx^2}\right)^2 dx \sim \kappa \left(\frac{h_o}{l_o^2}\right)^2 l_o \sim \kappa \frac{h_o^2}{l_o^3} \qquad (2)$$

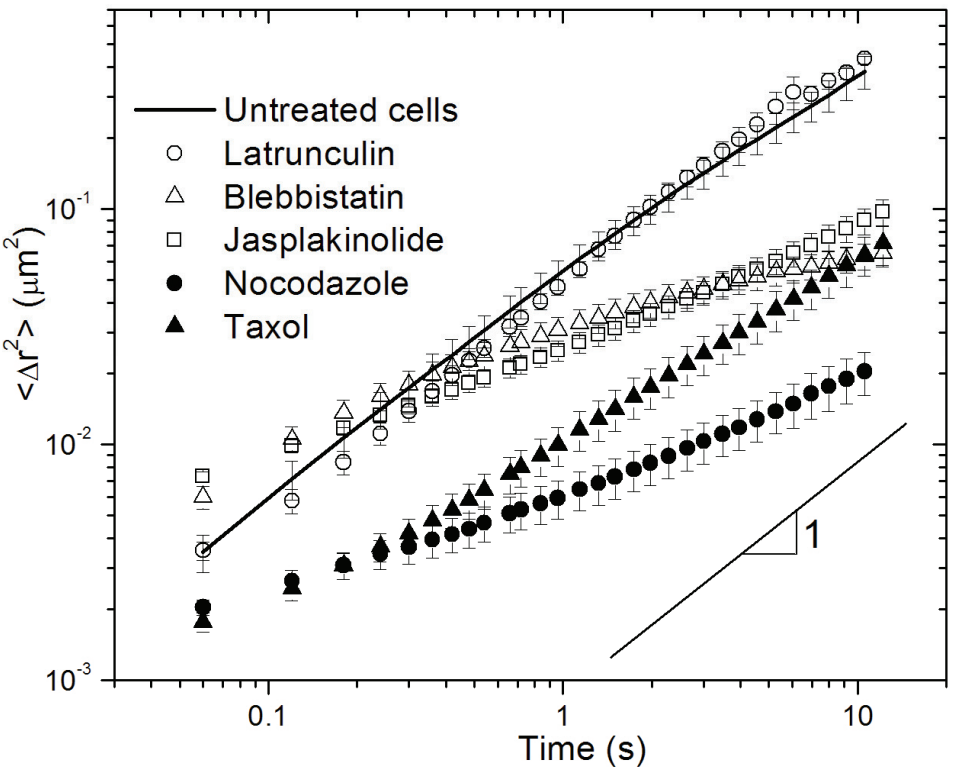

Figure 5: Effect of specific pharmacological interventions on the dynamics of endogenous granules in endothelial cells.

where κ is the bending rigidity and u(x) is the transverse deflection as a function of the axial coordinate x. At the point of incipient buckling, the surrounding elastic network resists the microtubule buckling as shown schematically by the springs in Fig. 6b. This competing elastic energy due to the surrounding matrix is given by

$$\int Gu^2 dx \sim Gh_o^2 l_o \tag{3}$$

At the onset of buckling this elastic energy of the matrix is of the order of the bending energy associated with the buckled microtubule i.e. $\kappa \frac{h_o^2}{l_o^3} \sim Gh_o^2 l_o$, which yields

$$l_o \sim (\kappa/G)^{1/4} \tag{4}$$

This estimate of l_o corresponds to the characteristic wavelength associated with constrained buckling (29). Using typical values of κ 10^{-23} Nm^2 and $G \approx 1$ kPa reported in the literature (28, 32) we obtain $l_o \approx 1$ μm. Now the active force, f, can be estimated from these elastic energies (either Eqn (2) or Eqn (3)) as

$$f \sim \frac{dE}{du} \sim \frac{\kappa h_o}{l_o^3} \tag{5}$$

By assuming that the EGs experience the transverse bending modes of the microtubules (see Fig. 6), we estimate h_o to be of the order of the root-mean squared displacement of EGs reported in Figure 2, i.e. $h_o \approx \sqrt{\langle \Delta r^2 \rangle} \approx 0.1 - 1 \mu m$. Thus, from Eqn (5), we obtain an estimate of active force $f \approx$ 1-10 pN, which is in accordance with typical forces exerted by motor-driven forces (33). Although this model, does not yield information on the specific nature of the active force it is likely that the source is either the actin-myosin contractility or microtubule polymerization forces, since both of them are capable of inducing microtubule bucking. Nevertheless, the model calculation indicates that microtubules play a crucial role in determining the dynamics of EGs.

According to the above model, using Eqns (4) and

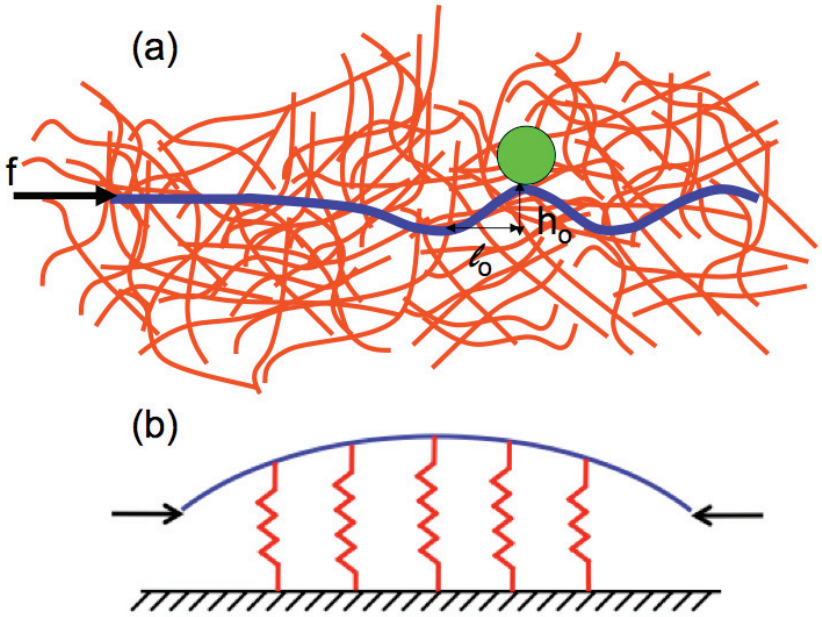

Figure 6: (a) A schematic (not to scale) showing a microtubule (in blue) embedded in an elastic medium (in red) undergoing short-wavelength bending due to a motor-driven force, f (modified from ref. 25). The endogenous granule (in green) is shown anchored to the microtubule. The characteristic lateral and transverse bending length scales are denoted by l_o and h_o respectively (b) A mechanical model showing how a localized bend in the microtubule could be elastically coupled to the surrounding network at the point of incipient buckling. Because of the coupling of the elastic medium, the characteristic wavelength for buckling will be shorter than the length of the rod.

(5), it can be shown that

$$\langle \Delta r^2 \rangle \sim f^2 / G^{3/2} \kappa^{1/2} \tag{6}$$

Eqn (6) implies that for a given microtubule stiffness, the amplitude of MSD of EGs is determined by two competing parameters - the magnitude of the active force, f, driving microtubule buckling and the elastic modulus, G, of the medium resisting buckling. Within this framework of the model, we interpret the results of drug interventions with AF and MT network reported in Figure 5. With the disruption of the actin network by latrunculin, the amplitude of MSD of EGs remains unchanged implying that– (i) the source of the active driving force, f, does not arise from actin-myosin contractility, but probably from microtubule polymerization forces. Thus acto-myosin contractility is not important in influencing the dynamics of EGs (ii) The modulus of the elastic medium resisting microtubule buckling is not determined by the actin network. Although this conclusion may appear surprising, recently, two-point microrheology of epithelial cells has also shown that the actin network does not contribute significantly to the intracellular rheology (34).

With blebbistatin and jasplakinolide, we observe a decrease in the MSD amplitude of EGs. Since we concluded earlier that active driving force for EGs arises from microtubule polymerization forces, this suggests that both myosin motor inhibition (by blebbistatin) and actin stabilization (by jasplakinolide) enhances the stiffness (G) of the underlying medium (c.f. Eqn (6)). Bursac et al. (6), also found reduced amplitude in the MSD under jasplakinolide intervention, of a bead attached to human airway smooth muscle cell cortex using magnetic twisting cytometry– an observation in line with our reasoning. van citters et al. (34), observed that upon blebbistatin intervention in epithelial cells, the MSD from two-point microrhe-

ology was largely unaffected – a result that is in contrast with our single-particle tracking observations and needs to be resolved.

With nocodazole and taxol treatments the dynamics of EGs slows down, but to a different degree. Immunofluorescence staining showed that the actin network was largely intact under the influence of these drugs, suggesting that they interfere with the microtubule polymerization forces (i.e. the active driving force, f) to a different extent.

4 Conclusions

Our results demonstrate that endogenous granules exhibit universal diffusive dynamics that is most likely driven by the microtubule bending dynamics due to active polymerization forces. We are led to this remarkable conclusion by the following key points of evidence (i) actin network disruption (by latrunculin) does not significantly affect the dynamics of EGs (ii) EG dynamics is quite sensitive to drugs (nocodazole and taxol) affecting microtubule network (iii) The dynamics of EGs under presumably passive conditions (temperature reduction to 24°C) is well described by a semiflexible polymer model that assumes EGs linked to microtubule network (iv) The magnitude of displacement exhibited by EGs in untreated cells is consistent with microtubule bending fluctuations driven by a motor-driven force.

In addition our findings lead to the following surprising implications. First, endogenous granules could be used as non-invasive microrheological probes for microtubule network dynamics in living cells. Second, literature studies that have been using endogenous granules to probe intracellular rheology might in fact be probing the mechanical properties of primarily the microtubule network rather than the entire living cytoskeleton. This could partly explain the wide variation in cell modulus reported by MPTM and other techniques such as atomic force microscopy and magnetic twisting cytometry (16).

Acknowledgement: We are grateful to D. Wirtz for advice on ballistic particle injection, V. Breedveld for the particle tracking code. We thank Andries van der Meer and Andre Poot for providing cell lines, cell culture training. SAV thanks Moumita Das for illuminating discussions on microtubule buckling. This research was supported by the Cell Stress program of the MESA+ Institute of Nanoechnology.

References

1. Kamm, R. D., Mofrad, M. R. K. (2006) Cytoskeletal mechanics: models and measurements (Cambridge University Press, New York).

2. Janmey, P. A., Weitz, D. A. (2004) *Trends Biochem. Sci.* 29, 365-370.

3. Heidemann, S. R., Wirtz, D. (2004) *Trends Cell Biol.* 14, 160-166.

4. Pollard, T. D. (2003) *Nature* 422, 741-745.

5. Balland, M., Richert, A., Gallet, F. (2004) *Eur. Biophys. J.* 34, 255-261.

6. Bursac, P., Lenormand, G., Fabry, B., Oliver, M., Weitz, D. A., Viasnoff, V., Butler, J. P., Fredberg, J. J. (2005) *Nat. Mater.* 4, 557–561.

7. Alcaraz, J., Buscemi, L., Grabulosa, M., Trepat, X., Fabry, B., Farre, R.,Navajas, D. (2003) *Biophys. J.* 84, 2071–2079.

8. Weihs, D., Mason, T. G., Teitell, M. A. (2006) *Biophys. J.* 91, 4296–4305.

9. Desprat, N., Richert, A., Simeon, J., Asnacios, A. (2005) *Biophys. J.* 88, 2224–2233.

10. Tseng, Y., Kole, T. P., Wirtz, D. (2002) *Biophys. J.* 83, 3162–3176.

11. Lau, A., Hoffman, B. D., Davies, A., Crocker, J. C., Lubensky, T. C. (2003) *Phys. Rev. Lett.* 91, 198101.

12. Yamada, S., Wirtz, D., Kuo, S. C. (2000) Biophys. J. 78, 1736–1747.

13. Yanai, M., Butler, J. P., Suzuki, T., Sasaki, H., Higuchi, H. (2004) Am. J. Physiol. Cell Physiol. 287, C603–C611.

14. Tolic-Norrelykke, I. M., Munteanu, E. L., Thon, G., Oddershede, L., Berg-Sorensen, K. (2004) Phys. Rev. Lett. 93, 078102.

15. Dangaria, J. H., Butler, P. J. (2007) Am. J. Physiol. Cell Physiol. 293, 1568-1575.

16. Hoffman, B. D., Massiera, G., van Citters, K. M., Crocker, J. C. (2006) *Proc. Natl. Acad. Sci. USA*. 103, 10259–10264.

17. Rogers, S. S., Waigh, T. A., Lu, J. R. (2008) Biophys. J. 94, 3313-3322.

18. Panorchan, P., Lee, J. S., Daniels, B. R., Kole, T. P., Tseng, Y., Wirtz, D. (2006) *Meth. Cell. Biol.* 83, 115-140.

19. Crocker, J. C., Grier, D. G. (1996) *J. Colloid Int. Sci.* 179, 298–310.

20. Caspi, A., Granek, R., Elbaum, M. (2000) *Phys. Rev. Lett.* 85, 5655–5658.

21. Pangarkar, C., Dinh, A. T., Mitragotri, S. (2005) *Phys. Rev. Lett.* 95, 158101.

22. Snider, J., Lin, F., Zahedi, N., Rodionov, V., Yu, C. C., Gross, S. P. (2004) *Proc. Natl. Acad. Sci. USA*. 101, 13204–13209.

23. Duits, M. H. G., Li, Y., Vanapalli, S. A., Mugele, F. (2009) Phys. Rev. E, 79, 051910.

24. Brangwynne, C. P., Koenderink, G. H., MacKintosh, F. C., Weitz, D. A. (2008) *Phys. Rev. Lett.* 100, 118104.

25. Brangwynne, C. P., MacKintosh, F. C., Weitz, D. A. (2007) *Proc. Natl. Acad. Sci. USA*. 104, 16128-16133.

26. Gittes, F., MacKintosh, F. C. (1998) *Phys. Rev. E.* 58, R1241-1244.

27. Caspi, A., Elbaum, M., Granek, R., Lachish, A., Zbaida, D. (1998) *Phys. Rev. Lett.* 80, 1106–1109.

28. Gittes, F., Mickey, B., Nettleton, J., Howard, J. (1993) *J. Cell. Biol.* 120, 923-934.

29. Brangwynne, C. P., MacKintosh, F. C., Kumar, S., Geisse, N. A., Talbot, J., Mahadevan, L., Parker, K. K., Ingber, D. E., Weitz, D. A. (2006) *J. Cell. Biol.* 173, 733-741.

30. Li, T. (2008) *J. Biomech.* 41, 1722-1729.

31. Das, M., Levine, A. J., MacKintosh, F. C. (2008) *Eur. Phys. Lett.* 84, 18003.

32. Fabry, B., Maksym, G. N., Bulter, J. P., Glogauer, M., Navajas, D., Fredberg, J. J. (2001) *Phys. Rev. Lett.* 87, 148102.

33. Howard, J., Hyman, A. A. (2003) *Nature*. 422, 753-758.

34. van Citters, K. M., Hoffman, B. D., Massiera, G., Crocker, J. C. (2006) *Biophys. J.* 91, 3946–3956.